

Super-resolution imaging as a method to study GPCR dimers and higher-order oligomers

Kim. C Jonas¹ and Aylin C. Hanyaloglu^{2*}

1. Centre for Medical and Biomedical Education, St George's, University of London, UK

2. Institute of Reproductive and Developmental Biology, Dept. Surgery and Cancer, Imperial College London, UK

*Corresponding author: a.hanyaloglu@imperial.ac.uk

Abstract

The study of G protein-coupled receptor (GPCR) dimers and higher order oligomers has unveiled mechanisms for receptors to diversify signaling and potentially uncover novel therapeutic targets. The functional and clinical significance of these receptor-receptor associations has been facilitated by the development of techniques and protocols, enabling researchers to unpick their function from the molecular interfaces, to demonstrating functional significance *in vivo*, in both health and disease. Here we describe our methodology to study GPCR oligomerization at the single molecule level via super-resolution imaging. Specifically, we have employed photoactivated localization microscopy, with photoactivatable dyes (PD-PALM) to visualize the spatial organization of these complexes to <10nm resolution, and the quantitation of GPCR monomer, dimer and oligomer in both homomeric and heteromeric forms. We provide guidelines on optimal sample preparation, imaging parameters and necessary controls for resolving and quantifying single molecule data. Finally, we discuss advantages and limitations of this imaging technique and its potential future applications to the study of GPCR function.

Keywords: GPCR, dimer, oligomer, super-resolution, PALM, single molecule imaging

1. Introduction

The ability of G protein-coupled receptors (GPCRs) to associate as dimers and higher-order oligomers with themselves (homomers), or distinct GPCRs (heteromers), has provided a mechanism to understand how these receptors can diversify their activity in different tissues, display altered pharmacological properties of distinct ligands and the side-effects of drugs targeting these receptors. Mechanistically, GPCR homomerization has been implicated in receptor trafficking and signal diversification and/or amplification [1, 2]. GPCR heteromerization, however, can essentially result in a unique receptor functional unit compared to their respective homomeric counterparts, with reported distinct cell surface targeting, pharmacology, G protein complement, and ligand-induced trafficking [2-5]. The road to studying these complexes, however, has been very rocky, and remains an area of debate, historically due to the lack of approaches applied to directly demonstrate a required function of these homomers and heteromers *in vivo* [6-9]. Thus, more recent studies have developed methodological strategies to demonstrate these complexes do indeed exist *in vivo* and are functionally relevant. Discussing the impact of GPCR homo and heteromerization to cell signaling and physiological/pathological function is outside the scope of this chapter, and thus we refer the reader to the following recent reviews that specifically describe the role of GPCR homomer and heteromers in receptor function *in vivo* and in disease [2, 4, 5].

Despite this progress there remain numerous outstanding questions on the molecular organization, and debate on the functional relevance of dimer versus oligomeric GPCR complex [10-13]. Indeed, with such a large family of receptors it is not inconceivable that distinct GPCRs may differ in their ability (or necessity) to form

such complexes. Even for a single GPCR it is likely there are roles for monomer, dimer and oligomer, rather than a model where a receptor is capable of only forming specific numerical complex, e.g. only dimers. The ability to provide molecular evidence to address these questions requires cross-disciplinary technology that can unpick the molecular interfaces, the full landscape of receptor complexes that are formed, and specific cellular and physiological roles of GPCR monomers, dimers, and oligomers. The development of a suite of single-molecule imaging approaches has contributed to unveiling the molecular organization of different GPCRs in cells and tissues, and its significance to cellular signaling. The approaches used have ranged from employing diffraction limited imaging and ultra-low receptor densities, but with superior temporal resolution, to unveil the dynamics of receptor-receptor associations at the plasma membrane; to those that break the light diffraction barrier of 200nm and employ super-resolution imaging at physiological densities of receptor, however, with as yet poor temporal resolution. The former approach has used total-internal reflection fluorescence microscopy (TIRF-M) combined with post-acquisition extrapolation of intensity data to visualize the dynamics of individual GPCRs associating as dimers and oligomers in live cells, in real time [14-17]. With such approaches receptors must be expressed at low densities (<10 molecules/ μm^2) to enable tracking and localization of individual molecules [18, 19]. This is due to the point spread function (PSF) of each molecule in typical diffraction-limited imaging. The fluorescence of a single molecule has a Gaussian-like intensity distribution; the PSF. PSFs have a radius of ~ 200 - 250 nm, and corresponds to the uncertainty of localization, or degree of spreading/blurring of a single point object, and is also impacted by the wavelength of emission and the light collection capacity of the objective [20]. If the PSF is sufficiently separated from other emitting species by a

distance greater than the resolution limit (~200–250 nm), this center can be located. This is why molecule density for diffraction-limited single molecule imaging is critical as all fluorophores are detected simultaneously, thus any overlap of the PSFs precludes super-resolution imaging and loss of structural detail [18]. Therefore, for visualization of GPCR dimers via this approach, the density must be less than a few molecules per μm^2 to enable visualization of individual receptors. Indeed, it has been optimized for enabling kinetic studies of individual receptor interactions rather than the detection of the overall landscape of GPCR monomers/dimers/oligomers [14-17]. The very high temporal resolution this technique affords, reveals the dynamic nature of these associations for certain GPCRs that would not be detectable by other real-time methods used to study protein-protein interactions, such as biophysical real-time techniques of BRET and FRET. We also refer the reader to recent reviews discussing all these distinct techniques for the study of GPCR di/oligomerization [18, 21]. Instead we will give a brief overview of super-resolution imaging with focus on photo-activated localization microscopy (PALM).

1.1 Photoactivated localization microscopy (PALM) to study GPCR oligomerization

Super-resolution approaches can map single molecules of labeled proteins down to <10 nm resolution, compared to conventional light microscopy that achieves ~200nm maximal resolution and encompasses a number of techniques including 2D and 3D localization microscopy techniques (PALM and stochastic optical reconstruction microscopy (STORM)), stimulated emission depletion (STED), structured illumination and light sheet microscopy, each of which have specific cellular applications in terms of spatial and temporal resolution capabilities, and ability for live cell imaging. With respect to studying GPCR oligomerization, only PALM out of the super-resolution

imaging approaches has been employed to date [22-24]. Localization microscopy approaches such as PALM and STORM provides the ability to image labeled molecules of interest due to stochastic switching of fluorescent probes, providing precisely localized single-molecule imaging [25, 26]. PALM involves the use of photoswitchable or photoactivatable fluorophores, which remain in the dark state until unmasked or activated by UV light, emitting fluorescence in a fluorophore-defined wavelength range and subsequently photobleached into the dark state (Figure 1). This activation occurs in a stochastic manner thus allowing for spatially separate detection of the activated molecules. These cycles are repeated until all fluorophores are activated and bleached into the dark state in order to ensure accurate and defined coordinate-specific detection of proteins (Figure 1).

The labeling of proteins for PALM require photoactivatable fluorophores, with many studies utilized tagging of proteins with large photoswitchable proteins, e.g., Dendra, Dendra2, mEosFP [25, 27]. For our studies utilizing PALM to study GPCR oligomerization at the cell surface, we employed photoactivatable dyes (PD) as they are brighter and more photostable than photoswitchable proteins, yet critically undergo irreversible activation and bleaching [28] to improve the accuracy of localizing and quantifying single receptors. An important distinction to highlight between prior single molecule studies employing TIRF-M to localization microscopy approaches such as PD-PALM, is that the latter enables localization of receptors expressed at much higher densities (~200 molecules/ μm^2 for PD-PALM vs 1-3 molecules for single molecule imaging/tracking techniques). An argument for both techniques in studying GPCR oligomerization under physiologically relevant

conditions have been made [14-18, 21]. For our prior studies with the luteinizing hormone receptor (LHR) we could localize and quantify between 2000 and 8000 receptors/cell, which are within the range previously reported for ovarian and testicular LHR (4000–20,000 receptors/cell) [24, 29, 30]. Certainly, there are GPCRs that are expressed at very low levels *in vivo*, although it is the temporal resolution of low-density/wide-field single molecule tracking techniques not afforded by localization microscopy that enables the study of receptor dimeric association and dissociation kinetics. Receptor density will be discussed further below in relation to quantitation of PD-PALM. Overall, by employing a super-resolution localization microscopy technique to study and identify LHR complexes not only provided a methodology to resolve single molecules beyond the diffraction limit of conventional microscopy, but enabled identification of individual LHR molecules at equivalent levels to those previously reported in endogenous tissues, rather than necessitating under-expression, or low labeling of receptors to enable resolution of single molecules.

2. Materials

2.1 Antibody labeled PD dyes

Selecting the best methodology for labeling your receptor of interest to ensure single-molecule detection is an important and nontrivial task, as a number of factors dictate the choice of probe. A probe needs to be bright, emitting sufficient photons to be easily localized, and distinguished from background, which all impact localization precision values of single molecules and thus the integrity of data obtained [31]. If GPCR heteromers are to be imaged via simultaneous dual-channel imaging, the emission spectra of your chosen probes also needs to be spectrally separated to

ensure minimal overlap and the correct identity of the localized molecules. For these reasons, we selected PDs for PALM imaging and we will subsequently refer to it as PD-PALM. When labeling your antibody with PDs ensuring a 1:1 stoichiometric labeling of probe receptor for single-molecule imaging is an obvious essential. For our studies, PDs were directly conjugated to primary HA and FLAG antibodies (purchased from Covance and Sigma-Aldrich respectively) were employed to visualize di/oligomers of two distinct mutant GPCRs at the cell surface. The CAGE 500 and CAGE 552 dyes, purchased from Abberior, are in the dark state and require uncaging via a UV light source to be activated. This uncaging is importantly irreversible. Antibodies were directly labeled with NHS-esters of these PDs, as directed by the manufacturer's instructions and protocols for labeling of antibodies/proteins with PDs (Abberior). It also is important to note that as the dye is in the dark state it is colorless and non-fluorescent. During handling and dye labeling it is very important to shield the dye from external light sources. Collect fractions before, during and after elution of label for analysis of the degree of labeling. This can be determined from the absorption spectrum of the labeled antibody and calculated based on a derivation of the Beer–Lambert law [24] using a nanodrop spectrophotometer. For our antibodies, the degree of labeling was determined as 1.0 ± 0.2 for FLAG-CAGE 500 and 1.3 ± 0.1 for HA-CAGE 552. Therefore, achieving an approximate 1:1 labeling of receptor: PD-conjugated antibody.

2.2 Sample preparation materials

For PD-PALM analysis of surface organization of GPCRs, imaging is also carried out under TIRF with a 1.45 numerical aperture. Therefore, selecting the right glass coverslip for imaging is needed to ensure that the best quality images are obtained. A high quality, no. 1.5 thickness cover-glass with minimal variation in thickness is

recommended for high numerical aperture objectives and super-resolution imaging. For our studies, we initially used 8-chamber well 1.5 borosilicate cover glass slides (Lab-tek) but have also employed 35mm dishes with 14mm diameter glass inserts (MatTek).

We have also optimized distinct blocking agents to minimize background and nonspecific binding of the FLAG and HA CAGE-labeled antibodies including; combinations of fish skin gelatin (1%) that is used in immunogold labeling for electron microscopy to reduce background (although the amount used may impact labeling efficiency) and fetal bovine serum (FBS), FBS alone, goat serum, a combination of goat serum and FBS. In our hands 10% FBS was used as both a blocking agent and to dilute the antibodies for incubation as this gave the least nonspecific background in HEK 293 cells.

PALM/PD-PALM employs fixed cells, although approaches to be able to use this technique in live cells is ongoing [32, 33]. This is because the photoactivatable dyes and photoswitchable proteins undergo stochastic excitation to ensure only a small subset of molecules are activated at any given time and repeated hundreds to tens of thousands of cycles in order to release and capture all unactivated molecules within the field of view. The fixative used for super-resolution imaging has been previously demonstrated to be very important as lateral diffusion of membrane proteins can still occur with conventional fixatives [34]. This study identified that simple addition of 0.2% glutaraldehyde to 4% paraformaldehyde exhibited the least lateral membrane diffusion of transmembrane proteins when compared to commonly

used fixatives, such as paraformaldehyde alone and methanol. Once fixed, cells are stored at 4 °C and imaged in PBS containing 1% sodium azide until imaged.

2.3 Microscope set-up

For our published studies [19, 24], we used a custom-adapted Inverted Axiovert 200 manual inverted wide-field fluorescent microscope (Zeiss, Germany) fitted with a commercial TIRF condenser kit (TILL Photonics GmbH, Germany), with a 1.45 numerical aperture 100× oil immersion objective. To activate uncaging of PDs, a polychrome light source was used at 390 nm (Polychrome IV, TILL Photonics GmbH, Uckfield, UK). Simultaneous dual channel imaging and photobleaching of activated FLAG-CAGE 500 and HA-CAGE 552 was conducted using 491- and 561-nm laser lines, respectively. Simultaneous imaging of CAGE 500 and 552 dyes was achieved using a beam splitter (Optosplit II, Andor) fitted with a T585lp dichroic and ET520-40 and ET632-60 emission filters (all Chroma). To minimize any environmental factors that may have impacted imaging, the microscope was enclosed in a plastic draft-proof system, always maintained at a constant temperature of 25 °C. Additionally, laser lines were always switched on at least 1 h before imaging to allow the system to stabilize and acclimatize prior to imaging. All of these measures ensured that minimal sample drift was observed when imaging. For capturing the images, a cooled electron multiplying charged-coupled device camera (EM-CCD; C9100-13, Hamamatsu) and Simple PCI software were used and time-lapse image series were taken, using an exposure time of 30 ms. For image registration and alignment of CAGE 500 and CAGE 552 generated images (required due to Optosplit-mediated simultaneous dual channel imaging), a combination of fiducial markers and grid images were used for post-acquisition alignment in Fiji ImageJ software. The fiducial

markers and grids acted as reference points to align the two channels post-acquisition.

There has been an increase in use of commercial systems for super-resolution imaging. We currently employ a Zeiss Elyra PS1 with an AxioObserver Z1 motorized inverted microscope. This microscope was custom designed to have two ECD cameras, to allow simultaneous dual-channel imaging without the necessity of an optisplit, and thus forgoing the need to align the two-channel images. Other advantages of this system include the automated nature of the TIRF and PALM imaging, plus certain features of the ZEN software that facilitate early image analysis, such as drift correction and signal to noise ratio values. In our hands, we would like to highlight that users must be still diligent to use sufficient laser power to ensure that PDs are fully bleached by the lasers within a single cycle, as our experience has been that more photoblinking/continuous PD activation over successive frames has been observed via commercial systems.

3. Methods

3.1 Cell labeling and image acquisition

Cells are seeded ideally between 30-60% confluency to enable to locate a sufficient number of adherent cells suitable for imaging in the TIRF plane. We suggest the following conditions to be optimized for labeling density, minimize background fluorescence, and prevent antibody- and fixation-induced artifacts. For each labeled antibody perform dilution curves, vary antibody incubation time and temperature of labeling conditions, in order to ensure labeling reaches saturation and to prevent under-labeling of the target protein. For our studies, we observed minimal

differences in the total percentage of detected associated molecules obtained when cells were fixed and subsequently labeled overnight at 4 °C, versus when PD-conjugated antibodies were incubated in live cells for 30 min at 37 °C and then subsequently fixed. These comparisons also demonstrate that the receptor di/oligomers could not be attributed to antibody-induced fixation. For assessing ligand-dependent changes, we therefore chose to label our cells live as steady-state labeling was reached using these conditions, and potential ligand-dependent changes could be carried out on pre-labeled cells [24]. Post-fixation, cells were stored at 4 °C and imaged in PBS containing 1% sodium azide. The use of an aqueous buffer or mounting fluid, such as PBS, can aid achieving the optimal TIRF angle.

For ensuring the optimal TIRF angle is selected for imaging, we have found it easiest to locate the coverslip, at the most acute TIRF angle, and locate the cell membrane (and labelled receptors), using a combination of adjusting the focal plane, and adjusting the TIRF angle. For image acquisition, there are a few key parameters to consider. The laser power used will determine the number of fluorophores activated, and thus the spatial separation achieved. However, this will also impact on the efficiency of photobleaching, therefore the laser power selected is a fine balance between achieving spatially separated fluorophores, whilst ensuring rapid photobleaching occurs. Image speed is also another consideration to be made. Imaging too quickly will often result in the same fluorophores being detected in multiple frames, however, imaging too slow will miss activated fluorophores, and so will impact on the information collected. Imaging speed is also dictated by the resolution of the camera. For our studies, we have found that imaging at 30 frames/second provides a good balance for these parameters. In terms of selecting

the number of photoactivation/bleaching cycles, this will be dictated by the number of fluorophores detected and localized, and is thus microscope, camera and acquisition set-up dependent. For our study, the number of photoactivation/photobleaching cycles selected was typically between 25,000–35,000 frames, to capture all labeled molecules and enable the assembly of the complete cell surface landscape of GPCR monomers/dimers/oligomers.

As discussed above, super-resolution imaging approaches can resolve higher densities of molecules, which for certain GPCRs is more physiologically relevant such as in our studies with LHR. However, whether imaging via diffraction-limited single particle tracking, or via super-resolution imaging, the density of receptor expression has been reported to impact the level and nature of certain forms of receptor complexes detected. We have reported that for LHR, increasing receptor density had little effect on the number of lower order receptor oligomers observed (dimers, trimers, and tetramers), but rather translated to differences in the number of higher order oligomers formed [19]. Likewise, prior studies using PALM and mEOS-tagged β 2-adrenergic receptor found an increase in the number of receptor oligomers with increasing receptor expression [23]. A similar observation was observed with diffraction limited single particle tracking and methodologies such as SpIDA (spatial intensity distribution analysis) with distinct GPCRs [16, 35]. Although they may be density-dependent, significance of these higher-order forms (>5 receptors) should not be overlooked. Some of these structures may represent signal microdomains, and certainly GPCR expression levels will dynamically change under both physiological and pathophysiological conditions. Further, given the reports of

GPCR heteromeric complexes that contain three distinct GPCRs [36, 37], and if each of these receptors also self-associate, then this may manifest itself in formation of very high order complexes.

Additional controls that can be employed for both experimental conditions employed and the chosen data analysis parameters (providing confidence in the ability of a given GPCR to form dimers and oligomers), is the use of a non-clustering transmembrane protein, or receptor. For our published studies, we utilized a member of the receptor tyrosine kinase family that is activated by macrophage colony stimulating factor (M-CSF), that basally is primarily monomeric. PD-PALM imaging of FLAG-tagged M-CSF receptor revealed that 85% of this receptor were monomers, with the majority of associating receptors residing as dimers. Further, coexpression of M-CSF with WT LHR detected minimal (<2%) heterocomplexes; demonstrating the specificity of the GPCR complexes observed by PD-PALM [24].

3.2 Post-acquisition analysis Part 1-Resolving single molecule data

Post-image acquisition, single molecules are assigned and identified via localization analysis to resolve the coordinates of individually activated CAGE-labeled molecules across all frames that are compressed into a single file. For our studies, individual receptors were identified using a freely available, open source ImageJ plug-in, QuickPALM [38]. The software identifies and localizes each fluorophore with subpixel accuracy across frame of the time-lapse series taken. Within the software, the parameters of analysis can be adjusted to refine the stringency of single

molecules identified and localized, e.g., image plane pixel size (155 nm for our system), the minimum signal to noise ratio of each experiment (typically 8, but reanalyzed for each experiment) and the full width, half maximum of single molecules (3). Each identified single-molecule is presented as a reconstruction map in image form, simultaneously generated as the analysis occurs, and a data set containing the localizations, or XY map coordinates, of each counted single molecule (Figure 3). For our on-going studies using the Zeiss Elyra set-up, we have continued to use QuickPALM for generation of XY coordinate maps. However, there are other Imagej plugins, such as ThunderSTORM that offer a good alternative for handling of super resolution PALM and STORM imaging data, offering processing abilities such as data rendering and drift correction.

Localization precision is the standard measure used for assessing the accuracy of localizing each detected fluorophore, and calculated via the theory of Thompson et al [39]. This takes into account several factors including the photon count for each molecule, noise, the full width half maximum of the observed PSF, and the camera pixel size. For our studies, localization precision was calculated to be approximately 20 nm. The resolution that we achieved was determined to be ~8 nm, based on the number of photons emitted by the CAGE dyes during activation, and the point spread function of the activated dye. Commercial systems also contain software to calculate the signal to noise ratio and localization precision obtained.

3.3 Quantification of GPCR monomers, dimers, and oligomers from PD-PALM datasets

PD-PALM generates multiple large data sets of localized receptor molecules (up to <8000 data points for every cell), therefore we developed custom software to quantify the number of receptors existing as monomers, dimers, and oligomers, but also to distinguish different receptor populations participating in homo- versus heterocomplexes [19, 24]. We developed a JAVA-based software that employed an adaptation of Getis and Franklin's nearest neighborhood approach (termed PD-Interpreter). This software is freely available to download at www.superimaging.org. The software was designed to identify a single-molecule and recursively searched within a chosen radius for further single molecules until no further molecules were found within the search radius (Figure 2). The software can then inform not only monomeric receptor or those participating in a dimer/oligomer, but also if an oligomer, the number of molecules in that oligomer. For dual color imaging and the study of heteromers, both information on homomeric and heteromeric complexes can be obtained (Figure 2). The radius that the nearest neighborhood analysis is conducted over is user selected, ranging from 10 nm to 100 nm. For our studies with the LHR we selected 50 nm. Although the LHR is a Class A GPCR, where sizes of the members of this family is ~6 nm [40, 41], this receptor belongs to the glycoprotein hormone receptor subfamily containing a very large extracellular domain. Further, considering the localization precision of our imaging (20 nm), the size of the PD-labeled antibody, ~20 nm in size, and the nature of the labeling means that the position of the dye on the antibody is unknown and will be heterogenous. The search radius of 50 nm gave the highest number of lower-order dimers, trimers, and tetramers when compared to radii of 20-100 nm (Figure 3). As

an added level of stringency to our quantitation, events within a radius of 10 nm of a “parent”-activated fluorophore were excluded from the analysis, however, such molecules were infrequent and typically resulted in only discounting approximately <1% of activated molecules. CAGE dyes undergo irreversible activation, however, in commercial systems we have found that photobleaching may be suboptimal. As such, we have developed an add-on algorithm that we run after generation of the XY coordinate tables (and before interrogation on di/oligomeric status) to eliminate molecules that occur in more than 1 frame. Grouping of molecules activated across more than 1 frame is also possible to do using the data rendering ability of the Zen software that operates that Zeiss Elyra.

Data from PD-Interpreter is outputted in pictorial and Excel spreadsheet form depicting self-associating and co-associating molecules. The spreadsheets contain a summary page with the total of self-associating and co-associating molecules. A breakdown of the number of each complex type, specifically the number of molecules within each complex, is also detailed within this summary page. Additional tabs contain the individual localization information on each assigned self-associating and co-associating complexes, and non-associating molecules. Data is also outputted as several different individual image files, initially depicting all molecules in the localization data sets from the two channels. From the analysis, co-localization plots are generated using blue and yellow colors to differentiate the two channel populations. A multi-color plot depicts complex size and represents clusters with 2 or more molecules each represented by different colors (both omitting non-associating molecules) (Figure 2).

When first quantifying PALM data sets we strongly suggest the use of theoretical or simulated datasets as controls. Excel can generate randomly dispersed data sets where one can vary the total numbers to simulate comparable receptor densities observed in experimentally obtained data sets. Theoretical data sets can then be subjected to the same analysis via PD-Interpreter software. By using this control in our studies with LHR, we demonstrated that the total percentage of associated molecules in our experimental data sets was greater than that for a randomly dispersed sample set [24].

4. Conclusions

Super-resolution imaging has enabled scientists to image structures and proteins in cells beyond the diffraction limit of standard fluorescent imaging approaches, including TIRF-M; unveiling an unprecedented depth of information to unveil the 'inner secrets' of how cells and proteins function. In the context of GPCR di/oligomerization, super-resolution imaging enables the study of these receptor complexes at densities to that found under physiological conditions. At present, there have been limited studies on the application of super-resolution imaging to study GPCR oligomerization, although these advanced imaging techniques are being increasingly applied to study other aspects of receptor function such as membrane trafficking [42-44]. Future applications of approaches such as PD-PALM that enable multi-channel imaging (>2) to visualize not only the receptor complexes, but their organization with the signaling machinery will enable assessment of current models that propose the asymmetric organization of receptor homo and heteromers with, for

example, different G proteins [1, 24, 45, 46]. The limitations at present of the current presented technique is the lack of temporal resolution, though these 'snap-shots' of GPCR organization provide the full detailed complement of receptor organization; improvements to apply live-cell PALM may require a reduction in the level of spatial resolution to achieve this. Further, extensions of PD-PALM to 3D PALM has the potential to analyze receptor complexes not just at the cell surface but also in distinct subcellular compartments, such as endosomes, Golgi and mitochondria that all have been reported to exhibit active GPCR/G protein signaling [47-50]. 3D super-resolution imaging will also facilitate single molecule resolution in tissue and multi-cellular *in vitro* systems such as organoids. Overall, we predict that this is only the start of the application of such techniques to the study of GPCRs, and in combination with other approaches such as molecular modeling, an unprecedented insight in to how these receptors function at the nano-scale.

Acknowledgements

This research was supported by supported by Biotechnology and Biological Sciences Research Council (BBSRC) project grant (BB/1008004/1), a BBSRC Sparking Impact Award and a Society for Endocrinology Early Career Grant.

References

1. Ferre, S., et al., G protein-coupled receptor oligomerization revisited: functional and pharmacological perspectives. *Pharmacol Rev*, 2014. **66**(2): p. 413-34.
2. Farran, B., An update on the physiological and therapeutic relevance of GPCR oligomers. *Pharmacol Res*, 2017. **117**: p. 303-327.
3. Franco, R., et al., Basic Pharmacological and Structural Evidence for Class A G-Protein-Coupled Receptor Heteromerization. *Front Pharmacol*, 2016. **7**: p. 76.
4. Gomes, I., et al., G Protein-Coupled Receptor Heteromers. *Annu Rev Pharmacol Toxicol*, 2016. **56**: p. 403-25.
5. Jonas, K.C. and A.C. Hanyaloglu, Impact of G protein-coupled receptor heteromers in endocrine systems. *Mol Cell Endocrinol*, 2017. **449**: p. 21-27.
6. Chabre, M. and M. le Maire, Monomeric G-protein-coupled receptor as a functional unit. *Biochemistry*, 2005. **44**(27): p. 9395-403.
7. James, J.R., et al., A rigorous experimental framework for detecting protein oligomerization using bioluminescence resonance energy transfer. *Nat Methods*, 2006. **3**(12): p. 1001-6.
8. Bouvier, M., et al., BRET analysis of GPCR oligomerization: newer does not mean better. *Nat Methods*, 2007. **4**(1): p. 3-4; author reply 4.
9. Salahpour, A. and B. Masri, Experimental challenge to a 'rigorous' BRET analysis of GPCR oligomerization. *Nat Methods*, 2007. **4**(8): p. 599-600; author reply 601.
10. Lambert, N.A. and J.A. Javitch, Rebuttal from Nevin A. Lambert and Jonathan A. Javitch. *J Physiol*, 2014. **592**(12): p. 2449.

11. Lambert, N.A. and J.A. Javitch, CrossTalk opposing view: Weighing the evidence for class A GPCR dimers, the jury is still out. *J Physiol*, 2014. **592**(12): p. 2443-5.
12. Bouvier, M. and T.E. Hebert, CrossTalk proposal: Weighing the evidence for Class A GPCR dimers, the evidence favours dimers. *J Physiol*, 2014. **592**(12): p. 2439-41.
13. Bouvier, M. and T.E. Hebert, Rebuttal from Michel Bouvier and Terence E. Hebert. *J Physiol*, 2014. **592**(12): p. 2447.
14. Hern, J.A., et al., Formation and dissociation of M1 muscarinic receptor dimers seen by total internal reflection fluorescence imaging of single molecules. *Proc Natl Acad Sci U S A*, 2010. **107**(6): p. 2693-8.
15. Kasai, R.S., et al., Full characterization of GPCR monomer-dimer dynamic equilibrium by single molecule imaging. *J Cell Biol*, 2011. **192**(3): p. 463-80.
16. Calebiro, D., et al., Single-molecule analysis of fluorescently labeled G-protein-coupled receptors reveals complexes with distinct dynamics and organization. *Proc Natl Acad Sci U S A*, 2013. **110**(2): p. 743-8.
17. Kasai, R.S. and A. Kusumi, Single-molecule imaging revealed dynamic GPCR dimerization. *Curr Opin Cell Biol*, 2014. **27**: p. 78-86.
18. Scarselli, M., et al., Revealing G-protein-coupled receptor oligomerization at the single-molecule level through a nanoscopic lens: methods, dynamics and biological function. *FEBS J*, 2016. **283**(7): p. 1197-217.
19. Jonas, K.C., I. Huhtaniemi, and A.C. Hanyaloglu, Single-molecule resolution of G protein-coupled receptor (GPCR) complexes. *Methods Cell Biol*, 2016. **132**: p. 55-72.

20. van der Merwe, P.A., et al., Taking T cells beyond the diffraction limit. *Nat Immunol*, 2010. **11**(1): p. 51-2.
21. Vischer, H.F., M. Castro, and J.P. Pin, G Protein-Coupled Receptor Multimers: A Question Still Open Despite the Use of Novel Approaches. *Mol Pharmacol*, 2015. **88**(3): p. 561-71.
22. Annibale, P., et al., Quantitative photo activated localization microscopy: unraveling the effects of photoblinking. *PLoS One*, 2011. **6**(7): p. e22678.
23. Scarselli, M., P. Annibale, and A. Radenovic, Cell type-specific beta2-adrenergic receptor clusters identified using photoactivated localization microscopy are not lipid raft related, but depend on actin cytoskeleton integrity. *J Biol Chem*, 2012. **287**(20): p. 16768-80.
24. Jonas, K.C., et al., Single molecule analysis of functionally asymmetric G protein-coupled receptor (GPCR) oligomers reveals diverse spatial and structural assemblies. *J Biol Chem*, 2015. **290**(7): p. 3875-92.
25. Betzig, E., et al., Imaging intracellular fluorescent proteins at nanometer resolution. *Science*, 2006. **313**(5793): p. 1642-5.
26. Owen, D.M., et al., Super-resolution imaging by localization microscopy. *Methods Mol Biol*, 2013. **950**: p. 81-93.
27. Williamson, D.J., et al., Pre-existing clusters of the adaptor Lat do not participate in early T cell signaling events. *Nat Immunol*, 2011. **12**(7): p. 655-62.
28. Belov, V.N., et al., Rhodamines NN: a novel class of caged fluorescent dyes. *Angew Chem Int Ed Engl*, 2010. **49**(20): p. 3520-3.
29. Luborsky, J.L., W.T. Slater, and H.R. Behrman, Luteinizing hormone (LH) receptor aggregation: modification of ferritin-LH binding and aggregation by

- prostaglandin F2 alpha and ferritin-LH. *Endocrinology*, 1984. **115**(6): p. 2217-26.
30. Dehejia, A., et al., Luteinizing hormone receptors and gonadotropic activation of purified rat Leydig cells. *J Biol Chem*, 1982. **257**(22): p. 13781-6.
 31. Patterson, G., et al., Superresolution imaging using single-molecule localization. *Annu Rev Phys Chem*, 2010. **61**: p. 345-67.
 32. Manley, S., J.M. Gillette, and J. Lippincott-Schwartz, Single-particle tracking photoactivated localization microscopy for mapping single-molecule dynamics. *Methods Enzymol*, 2010. **475**: p. 109-20.
 33. Deschout, H., et al., Complementarity of PALM and SOFI for super-resolution live-cell imaging of focal adhesions. *Nat Commun*, 2016. **7**: p. 13693.
 34. Annibale, P., et al., Identification of clustering artifacts in photoactivated localization microscopy. *Nat Methods*, 2011. **8**(7): p. 527-8.
 35. Ward, R.J., et al., Regulation of oligomeric organization of the serotonin 5-hydroxytryptamine 2C (5-HT_{2C}) receptor observed by spatial intensity distribution analysis. *J Biol Chem*, 2015. **290**(20): p. 12844-57.
 36. Sohy, D., et al., Hetero-oligomerization of CCR2, CCR5, and CXCR4 and the protean effects of "selective" antagonists. *J Biol Chem*, 2009. **284**(45): p. 31270-9.
 37. Navarro, G., et al., Interactions between intracellular domains as key determinants of the quaternary structure and function of receptor heteromers. *J Biol Chem*, 2010. **285**(35): p. 27346-59.
 38. Henriques, R., et al., QuickPALM: 3D real-time photoactivation nanoscopy image processing in ImageJ. *Nat Methods*, 2010. **7**(5): p. 339-40.

39. Thompson, R.E., D.R. Larson, and W.W. Webb, Precise nanometer localization analysis for individual fluorescent probes. *Biophys J*, 2002. **82**(5): p. 2775-83.
40. Mercier, J.F., et al., Quantitative assessment of beta 1- and beta 2-adrenergic receptor homo- and heterodimerization by bioluminescence resonance energy transfer. *J Biol Chem*, 2002. **277**(47): p. 44925-31.
41. Gurevich, V.V. and E.V. Gurevich, GPCR monomers and oligomers: it takes all kinds. *Trends Neurosci*, 2008. **31**(2): p. 74-81.
42. Eichel, K., D. Jullie, and M. von Zastrow, beta-Arrestin drives MAP kinase signalling from clathrin-coated structures after GPCR dissociation. *Nat Cell Biol*, 2016. **18**(3): p. 303-10.
43. Pons, M., et al., Phosphorylation of filamin A regulates chemokine receptor CCR2 recycling. *J Cell Sci*, 2017. **130**(2): p. 490-501.
44. Cooney, K.A., et al., Lipid stress inhibits endocytosis of Melanocortin-4 Receptor from modified clathrin-enriched sites and impairs receptor desensitization. *J Biol Chem*, 2017.
45. Navarro, G., et al., Quaternary structure of a G-protein-coupled receptor heterotetramer in complex with Gi and Gs. *BMC Biol*, 2016. **14**: p. 26.
46. Ferre, S., The GPCR heterotetramer: challenging classical pharmacology. *Trends Pharmacol Sci*, 2015. **36**(3): p. 145-52.
47. Irannejad, R., et al., Functional selectivity of GPCR-directed drug action through location bias. *Nat Chem Biol*, 2017. **13**(7): p. 799-806.
48. Irannejad, R., et al., Conformational biosensors reveal GPCR signalling from endosomes. *Nature*, 2013. **495**(7442): p. 534-8.

49. Suofu, Y., et al., Dual role of mitochondria in producing melatonin and driving GPCR signaling to block cytochrome c release. *Proc Natl Acad Sci U S A*, 2017. **114**(38): p. E7997-E8006.
50. Godbole, A., et al., Internalized TSH receptors en route to the TGN induce local Gs-protein signaling and gene transcription. *Nat Commun*, 2017. **8**(1): p. 443.

Figure Legends

Figure 1. Principles of PD-PALM. Schematic to demonstrate the principles of PD-PALM utilizing simultaneous dual-color imaging of CAGE 500- and 552-labeled receptors. CAGE 500 and 552 dyes are stochastically “uncaged” by UV, excited, and photo-bleached using 491- and 561-nm lasers, respectively. This is repeated through multiple cycles until all fluorophores are activated and bleached. A representative reconstructed PD-PALM image of an individual GPCR heterotrimer is highlighted. Scale bar = 50 nm. Adapted from [24].

Figure 2. Workflow of PD-PALM imaging and quantitation of GPCR oligomers.

Following image acquisition, reconstruction and extraction of single molecule coordinates is carried out via the Fiji/ImageJ plugin QuickPALM. These coordinates. Data tables containing x-y particle localization coordinates were generated, and two-dimensional coordinates were determined. To analyze the number of associated receptor molecules from the x-y particle localization coordinates, a custom Java application was designed (PD-Interpreter). A second order Getis Franklin neighborhood analysis was conducted, using defined search radii, to determine the degree of both homomeric associations within an individual channel and heteromeric associations across channels. To identify monomers, dimers and oligomers, the software recursively searches at a specific radius (here 50 nm) from each associating molecule until no further associating molecules were identified within the allotted search radius. Once an associating group of molecules is assigned, the composition of the di/oligomer is identified and omitted from further searches, so that molecules were not double counted. Data can be represented in the form heat maps,

with individual colors depicting different numbers of associating molecules and outputted in Excel format for graph presentation. Adapted from [24].

Figure 3. Percentage of GPCR dimers, trimers, and tetramers at varying search radii. Following reconstruction of PD-PALM images in QuickPALM and extraction of xy coordinates for all single receptors imaged, the number of dimers and oligomers were quantitated with varying radii (20-100 nm). From this analysis, a search radius of 50 nm was selected as it identified the highest number of lower order associating complexes i.e. dimers/trimers/tetramers. Data obtained from HEK 293 cells stably expressing HA-tagged mouse LHR. All data points represent the mean \pm S.E. of 10–12 individual cells, $n = 3$. From [24].

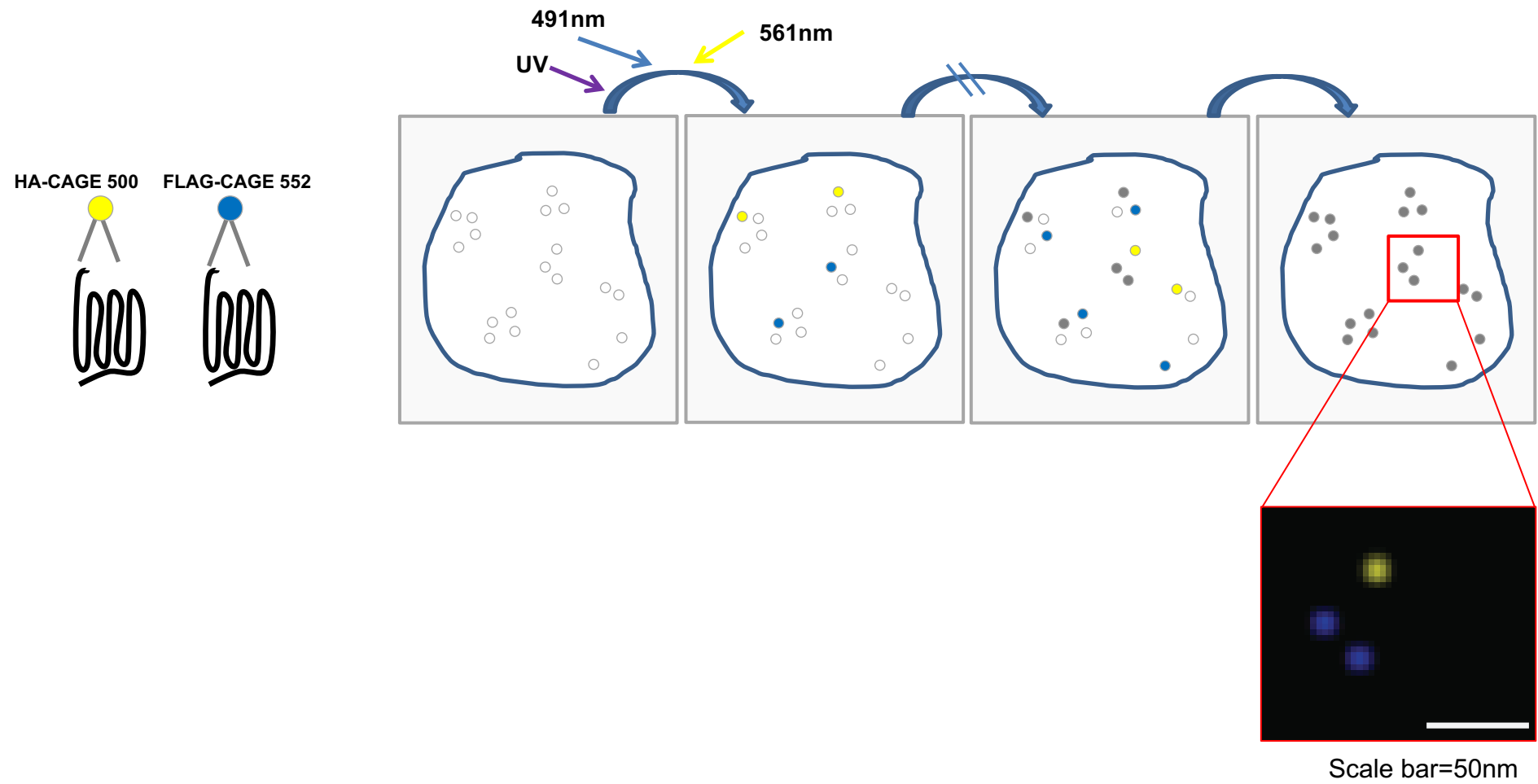
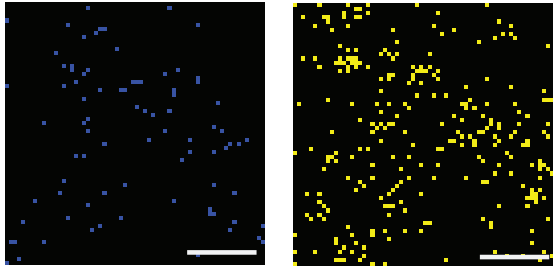


Figure 1. Jonas & Hanyaloglu

PD-PALM



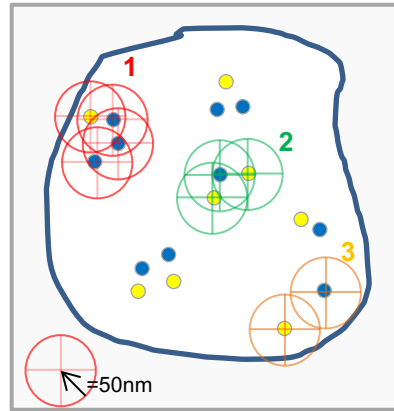
Scale bar=500nm

QuickPalm



Intensity	X [nm]	Y [nm]	Z [nm]	Left	Right	Up	Down	East	Symmet	Width	Frame Number				
1	400	101.4427	58.2096	10168.37	10169.90	0	1.28690	0.00021	0.00021	1.00054	0.17170	0.12344	0.00056	23	
1	2	176	44.4523	249.1041	14103.25	14103.41	0	1.402077	1.2781	1.00424	1.00116	0.21412	0.12012	33	
6	3	946	101.1241	101.1497	10121.41	10121.47	0	0.1942	0.1942	0.00000	1.22822	0.00000	0.20077	0.00000	23
4	177	140.4434	249.1078	14104.34	14103.76	0	1.121204	1.12121	1.013062	1.137816	0.018156	0.201289	0.131070	27	
5	200	101.1497	101.1241	10121.47	10121.41	0	1.00174	1.00174	1.00000	1.22822	0.00000	0.20077	0.00000	24	
7	6	164	101.6477	55.1460	10166.77	10164.62	0	1.121114	0.00151	0.041517	1.401346	0.47096	0.620554	0.071044	24
7	100	101.6477	55.1460	10166.77	10164.62	0	1.121114	0.00151	0.041517	1.401346	0.47096	0.620554	0.071044	24	
7	140	101.6477	55.1460	10166.77	10164.62	0	1.121114	0.00151	0.041517	1.401346	0.47096	0.620554	0.071044	24	
7	180	101.6477	55.1460	10166.77	10164.62	0	1.121114	0.00151	0.041517	1.401346	0.47096	0.620554	0.071044	24	
7	220	101.6477	55.1460	10166.77	10164.62	0	1.121114	0.00151	0.041517	1.401346	0.47096	0.620554	0.071044	24	
7	260	101.6477	55.1460	10166.77	10164.62	0	1.121114	0.00151	0.041517	1.401346	0.47096	0.620554	0.071044	24	
7	300	101.6477	55.1460	10166.77	10164.62	0	1.121114	0.00151	0.041517	1.401346	0.47096	0.620554	0.071044	24	
7	340	101.6477	55.1460	10166.77	10164.62	0	1.121114	0.00151	0.041517	1.401346	0.47096	0.620554	0.071044	24	
7	380	101.6477	55.1460	10166.77	10164.62	0	1.121114	0.00151	0.041517	1.401346	0.47096	0.620554	0.071044	24	
7	420	101.6477	55.1460	10166.77	10164.62	0	1.121114	0.00151	0.041517	1.401346	0.47096	0.620554	0.071044	24	
7	460	101.6477	55.1460	10166.77	10164.62	0	1.121114	0.00151	0.041517	1.401346	0.47096	0.620554	0.071044	24	
7	500	101.6477	55.1460	10166.77	10164.62	0	1.121114	0.00151	0.041517	1.401346	0.47096	0.620554	0.071044	24	
7	540	101.6477	55.1460	10166.77	10164.62	0	1.121114	0.00151	0.041517	1.401346	0.47096	0.620554	0.071044	24	
7	580	101.6477	55.1460	10166.77	10164.62	0	1.121114	0.00151	0.041517	1.401346	0.47096	0.620554	0.071044	24	
7	620	101.6477	55.1460	10166.77	10164.62	0	1.121114	0.00151	0.041517	1.401346	0.47096	0.620554	0.071044	24	
7	660	101.6477	55.1460	10166.77	10164.62	0	1.121114	0.00151	0.041517	1.401346	0.47096	0.620554	0.071044	24	
7	700	101.6477	55.1460	10166.77	10164.62	0	1.121114	0.00151	0.041517	1.401346	0.47096	0.620554	0.071044	24	
7	740	101.6477	55.1460	10166.77	10164.62	0	1.121114	0.00151	0.041517	1.401346	0.47096	0.620554	0.071044	24	
7	780	101.6477	55.1460	10166.77	10164.62	0	1.121114	0.00151	0.041517	1.401346	0.47096	0.620554	0.071044	24	
7	820	101.6477	55.1460	10166.77	10164.62	0	1.121114	0.00151	0.041517	1.401346	0.47096	0.620554	0.071044	24	
7	860	101.6477	55.1460	10166.77	10164.62	0	1.121114	0.00151	0.041517	1.401346	0.47096	0.620554	0.071044	24	
7	900	101.6477	55.1460	10166.77	10164.62	0	1.121114	0.00151	0.041517	1.401346	0.47096	0.620554	0.071044	24	
7	940	101.6477	55.1460	10166.77	10164.62	0	1.121114	0.00151	0.041517	1.401346	0.47096	0.620554	0.071044	24	
7	980	101.6477	55.1460	10166.77	10164.62	0	1.121114	0.00151	0.041517	1.401346	0.47096	0.620554	0.071044	24	
7	1000	101.6477	55.1460	10166.77	10164.62	0	1.121114	0.00151	0.041517	1.401346	0.47096	0.620554	0.071044	24	

PD-Interpreter



1= heterotetramer
2= heterotrimer
3= monomer

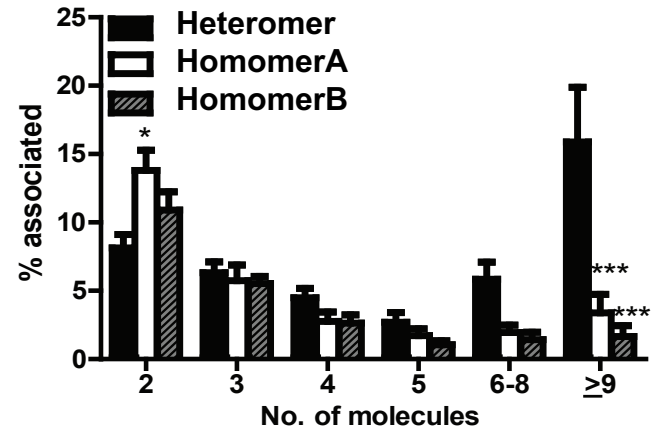
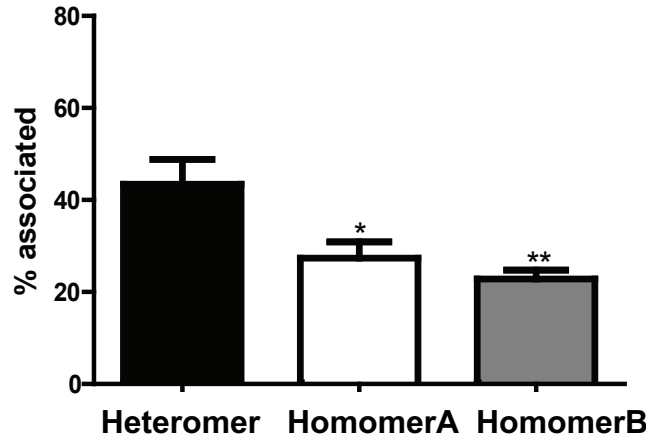
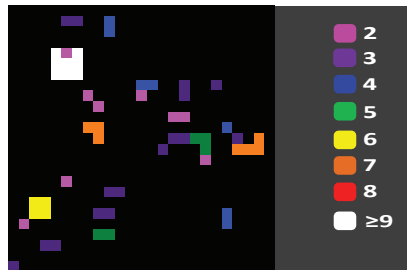


Figure 2. Jonas & Hanyaloglu

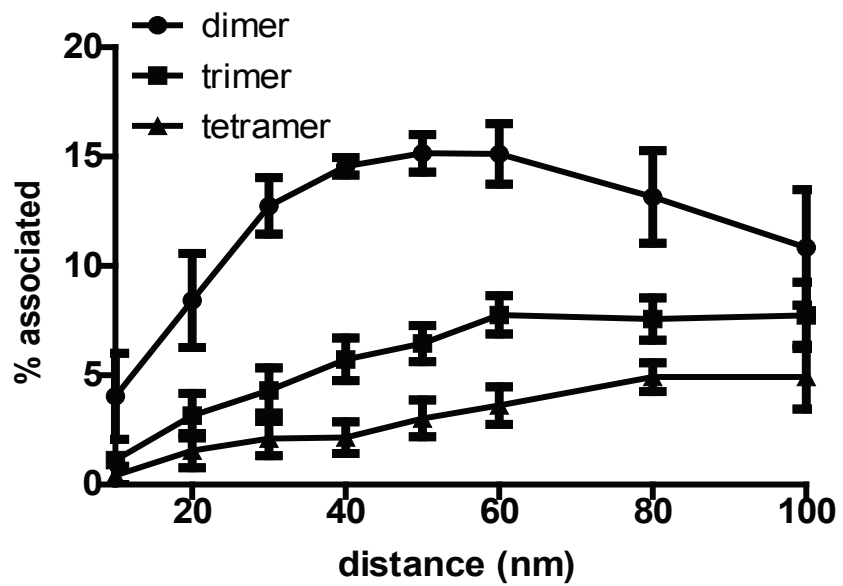


Figure 3. Jonas & Hanyaloglu